Title

2D IR spectroscopy reveals the role of water in the binding of channel-blocking drugs to the influenza M2 channel

Journal

The Journal of Chemical Physics, 140(23)

ISSN

0021-9606

Authors

Ghosh, Ayanjeet
Wang, Jun
Moroz, Yurii S
et al.

Publication Date

2014-06-21

DOI

10.1063/1.4881188

Peer reviewed

2D IR spectroscopy reveals the role of water in the binding of channel-blocking drugs to the influenza M2 channel

Ayanjeet Ghosh,[1,a)] Jun Wang,[2] Yurii S. Moroz,[3] Ivan V. Korendovych,[3] Martin Zanni,[4] William F. DeGrado,[2] Feng Gai,[1,a)] and Robin M. Hochstrasser[1,b)]
[1]*Department of Chemistry, University of Pennsylvania, Philadelphia, Pennsylvania 19104, USA*
[2]*Department of Pharmaceutical Chemistry, University of California San Francisco, San Francisco, California 94143, USA*
[3]*Department of Chemistry, Syracuse University, Syracuse, New York 13244, USA*
[4]*Department of Chemistry, University of Wisconsin, Madison, Wisconsin 53706, USA*

(Received 20 December 2013; accepted 21 May 2014; published online 19 June 2014)

Water is an integral part of the homotetrameric M2 proton channel of the influenza A virus, which not only assists proton conduction but could also play an important role in stabilizing channel-blocking drugs. Herein, we employ two dimensional infrared (2D IR) spectroscopy and site-specific IR probes, i.e., the amide I bands arising from isotopically labeled Ala30 and Gly34 residues, to probe how binding of either rimantadine or 7,7-spiran amine affects the water dynamics inside the M2 channel. Our results show, at neutral pH where the channel is non-conducting, that drug binding leads to a significant increase in the mobility of the channel water. A similar trend is also observed at pH 5.0 although the difference becomes smaller. Taken together, these results indicate that the channel water facilitates drug binding by increasing its entropy. Furthermore, the 2D IR spectral signatures obtained for both probes under different conditions collectively support a binding mechanism whereby amantadine-like drugs dock in the channel with their ammonium moiety pointing toward the histidine residues and interacting with a nearby water cluster, as predicted by molecular dynamics simulations. We believe these findings have important implications for designing new anti-influenza drugs. © *2014 AIP Publishing LLC*. [http://dx.doi.org/10.1063/1.4881188]

I. INTRODUCTION

Influenza virus infections present an annual widespread epidemic,[1] and are the sixth leading cause of death among adults in the US. Influenza inhibitors include a class of small molecule drugs[2] that target the M2 protein, a proton selective transmembrane channel that is an integral part of the viral envelope and plays a key role in viral reproduction.[3–5] While it is well recognized that water, which is an integral part of the M2 proton channel, is required for assisting proton conduction, its role in drug binding is not well understood. The homotetrameric M2 channel is known to undergo a pH dependent conformational transition that underlies its proton gating and conductance activity.[6–16] The tetrad formed by the His37 residues is believed to play a key role in controlling the transition between the closed and open states, via a protonation/deprotonation mechanism.[10,12,13,17–20] At neutral pH the equilibrium distribution of conformers is dominated by the doubly protonated (or +2) state of the His37 tetrad, while at acidic pH the +3 state is also formed. Protons transit through the M2 channel via a mechanism that involves: (1) protonation of the +2 state to generate the +3 state, (2) redistribution of the conformational equilibrium to favor opening of the Trp41 "gate,"[21] and (3) release of a proton to the viral interior. Thus, the channel oscillates between the +2 and +3 states as it conducts protons. Molecular dynamics (MD) and Quantum mechanics/Molecular mechanics (QM/MM) calculations[22] have further indicated that the water molecules inside a closed M2 channel tend to cluster in defined positions, tethered by interactions with His37 and the carbonyl groups lining the channel.[23]

Amantadine and rimantadine are a class of adamantane-based influenza inhibitors that lock the M2 channel in a non-conducting state by a mixed mechanism involving steric occlusion, pKa shifting, and freezing of the conformational ensemble to favor non-conducting states.[3,24,25] However, mutant strains of the virus have developed resistance toward this class of drugs, such that the Centers for Disease Control and Prevention (CDC) has advised against its use (details at: http://www.cdc.gov/flu/professionals/antivirals/links.htm). The design of inhibitors that target the M2 channel of such mutant strains has therefore become an important challenge in new drug development that requires a deeper understanding of the microscopic mechanism of drug-docking and proton translocation. A recent theoretical study indicated that square planar arrays of carbonyl groups in the channel stabilize the mobile hydrated ammonium groups of a methyl-ammonium ligand.[22] Consistently, nuclear magnetic resonance (NMR) measurements also indicate that amantadine situates in the M2 channel in a manner where with its hydrophobic adamantyl group is docked against the V27 residues and the amino end projects toward the intraviral C-terminal domain.[24,26] MD simulations[23,27] further show that the amino group of amantadine is solvated by four water molecules (Figure 1) in a square

[a)]Authors to whom correspondence should be addressed. Electronic addresses: ayanjeet@sas.upenn.edu and gai@sas.upenn.edu. Telephone: 215-573-6256. Fax: 215-573-2112.
[b)]Deceased.

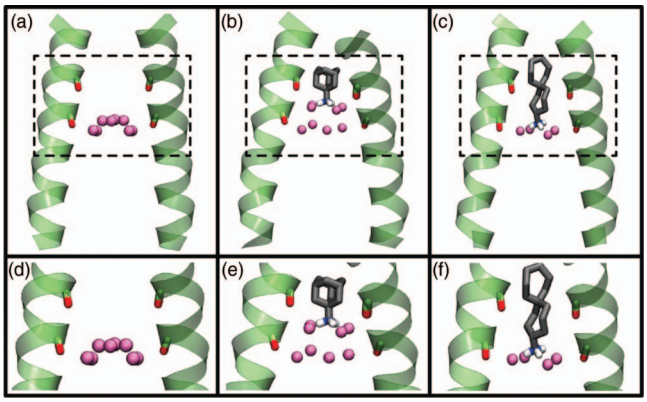

FIG. 1. (a) Crystal structure[28] of the M2 channel showing the water structure near Gly34. The water oxygen atoms are shown in pink. The Ala30 and Gly34 amide units, which interact with the water, are also shown. (b) Snapshot from MD trajectories[23] showing the binding of amantadine in the M2 channel in the closed state. (c) Orientation of the ammonium group for the more elongated and bulky 7,7-spiran amine, as shown by MD simulations.[23] (d), (e), and (f) are represent the same as (a), (b), and (c), respectively, but are zoomed in on the area marked by the dashed rectangle.

pyramidal arrangement which is stabilized through hydrogen bonds with a carbonyl box formed by the four carbonyl groups of Ala30. Furthermore, MD simulations predict the existence of another square pyramidal water cluster that is stabilized by the Gly34 carbonyls one helical turn down the channel. This tetrad of water molecules has also been observed in X-ray crystallographic measurements.[28] Guided by these previous observations and predictions, a set of ammonium-containing spiro compounds has recently been designed to target the M2 channel with the expectation that drug binding would be significantly stabilized through interactions with the aforementioned carbonyl tetrads and the distinctive water clusters in the channel.[23] While experimental results[23] indeed indicate that this series of spiro compounds has high affinity toward the M2 channel, MD simulations[23] suggest that the spiro compound binds in an amantadine-like mode deeper within the channel, docking itself in the pore through interactions with the water cluster near Gly34 (Figure 1(c)). Hence, the structural distribution and dynamics of the channel water should reflect the binding mechanism of the drug.

To provide new insight into the role of water in mediating drug-M2 interactions, we employ two dimensional infrared (2D IR) spectroscopy. The amide I′ bands of proteins are well established markers of solvation, because the electric fields of the water alter the vibrational frequency of the residues. When used in conjunction with isotope labeling, one can obtain residue-by-residue information on hydration dynamics, as has been demonstrated with experiment and theory over the past decade on several membrane protein domains, including CD3zeta, M2, and ovispirin.[29–32] In this study, we use a double mutant (D44N, R45A)[31,33,34] of the transmembrane domain of the M2 channel, with the pore lining carbonyls of its Ala30 and Gly34 residues isotopically labeled (i.e., $^{12}C{=}^{16}O$ to $^{13}C{=}^{18}O$) to serve as site-specific IR probes.[35–38] The use of this double mutant avoids any potential complexity arising from the 2D IR signals of arginine and aspartic acid, which overlap with those of the $^{13}C{=}^{18}O$ groups. In addition, 2D IR measurements are carried out at both pH 7, where the +2 state predominates, and pH 5, where the +3 state predominates, and with and without the presence of two amine-containing channel-blocking drugs, namely, rimantadine and 7,7-spiran amine. Our results show that upon binding of an amantadine-like drug the spectral diffusion of these IR probes becomes distinctively faster, indicating that the channel water becomes more mobile. This finding is interesting as it suggests that drug-binding leads to an increase of the entropy of the channel water, a thermodynamic outcome that favors the drug-M2 interaction. In addition, our data support a binding mechanism whereby amantadine-like drugs dock in the channel with their ammonium moiety pointing toward the histidine residues and interacting with a nearby water cluster, as predicted by computer simulations.

II. MATERIALS AND METHODS

A. Peptide synthesis

Peptides were synthesized by introducing $^{13}C{=}^{18}O$ labels on Gly34 and Ala30 into the transmembrane region (residues 22-46) of the Influenza A M2 protein (sequence: $SSNPLVVAA_{30}SIIG_{34}ILHLILWILNAL$). N-Fmoc-1-$^{13}C{=}^{18}O$ labeled amino acids (Ala, Gly) were prepared using the corresponding N-Fmoc-1-^{13}C labeled amino acids (99% ^{13}C, Cambridge Isotope Laboratories, Andover, MA) and $H_2{}^{18}O$ according to the literature procedure,[39] allowing for at least 90% isotopic enrichment in ^{18}O. The products were characterized by mass spectrometry: For $^{13}C{=}^{18}O$ labeled Fmoc-Alanine, ESI-MS: m/z (M+H+): 317.3 (calculated), 317.3 (found); for $^{13}C{=}^{18}O$ labeled Fmoc-Glycine, ESI-MS: m/z (M+H+): 303.3 (calculated), 303.3 (found). The peptides were synthesized by manual fluorenylmethyloxycarbonyl (Fmoc) solid phase synthesis on a 0.1 mmol scale using a Rink Amide-MBHA resin (GL Biochem) with a substitution level of 0.61 mmol/g using a procedure optimized for hydrophobic sequences.[40] Activation of the free amino acids (5-fold excess, 1.5-fold excess in case of N-Fmoc-1-$^{13}C{=}^{18}O$ labeled amino acids) was achieved with 0.95 equivalents (relative to the amino acid) of 1H-benzotriazolium 1-[bis(dimethylamino)methylene]-5-chloro-hexafluorophosphate (1-)-3-oxide (HCTU) in the presence of 10 equivalents of diisopropylethylamine (DIEA); a 5% (v/v) piperazine solution was used for deprotection. The coupling and deprotection steps were done at 60 °C for all residues expect His, which was coupled at room temperature. The reaction solvent contained 25% dimethylsulfoxide (DMSO) and 75% N-methylpyrrolidone (NMP) (HPLC grade, Aldrich). Side chain deprotection and simultaneous cleavage from the resin were performed using a mixture of trifluoroacetic acid (TFA)/H_2O/triisopropyl silane (TIS) (95:2.5:2.5, v/v) at room temperature for 2 h. The reaction mixture was filtered and the filtrate volume was reduced by ∼50% using a stream of nitrogen. Addition of cold diethyl ether (−20 °C) to the filtrate yielded crude product as a precipitate. The precipitate was washed with cold diethyl ether three times and dried in a stream of nitrogen. The crude peptides were purified on a reverse phase HPLC system (Varian ProStar 210) with

a C4 preparative column (Vydac) using a linear gradient of buffer A (0.1% TFA in Millipore water) and buffer B (6:3:1 2-propanol:acetonitrile:water) containing 0.1% TFA, starting from 40% of solvent B. Both peptides were characterized by ESI-MS showing identical mass: ESI-MS: m/z (M+2H+): 1321.6 (calculated), 1321.6 (found); (M+3H+): 881.1 (calculated), 881.1 (found). After purification the peptides were at least 95% pure by HPLC. Stock solutions of peptides in trifluoroethanol (TFE) were prepared from the lyophilized powder. Concentrations of the stock solutions of the peptides were determined by UV/Vis absorbance spectroscopy ($\varepsilon_{280} = 5500\ M^{-1}\ cm^{-1}$) using an Agilent 8453 spectrophotometer.

B. Preparation of 2D IR samples

The samples for 2D-IR measurements were prepared by mixing appropriate volumes of the stock solutions of the peptides with 100 mM stock solutions of dodecyl phosphatidylcholine (DPC) in TFE and 20 mM stock solutions of the appropriate drug in TFE. The solvent was subsequently removed in a stream of nitrogen and the resulting films were dried *in vacuo* for 30 min to remove residual organic solvent. The peptide-drug-detergent film was then dissolved in 200 ml of CD_3OD and kept for 30 min before the solvent was removed in a stream of nitrogen. The resulting peptide-drug-detergent film was dried *in vacuo* to ensure complete removal of TFE and deuterated methanol, and redissolved in 75 ml of the appropriate buffer solution (20 mM cacodylate pH = 5.0 or 20 mM phosphate pH = 7.0) containing 100 mM NaCl. The samples were then lyophilized. 15 ml of D_2O was added immediately prior to the experiment to produce samples with the following composition: [peptide] = 10 mM, [DPC] = 350 mM, [buffer] = 100 mM, and [NaCl] = 500 mM.

C. 2D IR measurements

The experimental scheme for collection of 2D IR spectra has been detailed elsewhere.[35,41,42] Fourier-transform limited 85-fs pulses with a center frequency of ∼1585 cm^{-1} were used for the experiments. The samples were irradiated with a sequence of three pulses, and the signal in the phase-matched direction $-k_1 + k_2 + k_3$ was collected by heterodyning it with a local oscillator pulse that preceded the signal pulse by a fixed interval of ∼1 ps. The signal and local oscillator pulses were combined at the focal plane of a monochromator having a 64-element liquid nitrogen cooled MCT array detector (InfraRed Associates). In general, the experiment yields a signal $S(\tau,T,t)$ that is a function of the time intervals between the pulses which is Fourier-transformed along τ and t into the 2D spectra $S(\omega_\tau, \omega_t, T)$ for each population interval T. Following Fayer and co-workers,[43] phasing of the 2D spectra was carried out by matching the projection of the 2D IR spectrum onto the ω_t axis with the corresponding simulated pump-probe spectrum which was obtained from the corresponding linear IR spectrum. In addition, 2D spectra obtained at different waiting times were checked for self-consistency by comparing their projections. The correctness of this phasing procedure was further checked by comparing the corrective phase factors thus obtained to those extracted from matching the projection of the 2D IR spectra of the Ala30 labeled M2 at pH 7 to the corresponding pump-probe spectrum.[44] To extract the vibrational lifetimes from 2D spectra, evolution of the positive (0→1) peak signal with the waiting time was used. For comparison, the vibrational lifetime for the A30 labeled, drug free channel at pH 7 was also evaluated by tracking the decay of the volume under the positive peak with the waiting time. The two methods yield lifetimes that differ by less than 15%, thus showing the equivalence of the two approaches. For extracting the diagonal to cross peak ratios from 2D spectra, the following procedure was followed. For each 2D IR spectrum (at a given waiting time), the frequency positions and $\{\omega_\tau{}^B, \omega_t{}^B\}$ of the diagonal peaks were determined. Then the intensities of the diagonal peak at $\{\omega_\tau{}^A, \omega_t{}^A\}$ and the cross peak at $\{\omega_\tau{}^A, \omega_t{}^B\}$ were recorded. This procedure was repeated for all waiting times, and the obtained cross peak:diagonal peak ratios were fit to Eq. (4). Due to overlap of the two diagonal peaks, the cross peak region exhibits small but finite signal at $T = 0$. The signal at $T = 0$ was subtracted from the ratio at all waiting times to get $\Delta S_{cross}/S_{diagonal}$, which reflects only the growth kinetics.

D. Mutation of the M2 sequence

A recent 2D IR study[33] has shown that energy transfer between two degenerate CN stretching modes of the guanidyl side chain of arginine, the infrared transitions of which overlap spectrally with isotopically edited amides, can occur on the timescale of a few picoseconds. Moreover, the carboxylate sidechains of glutamic and aspartic acids also absorb in the same spectral range as isotopically labeled amide modes. The M2 transmembrane domain has one arginine (R45) and an aspartic acid (D44) in its sequence. To circumvent the background signals of these residues, a mutated sequence of M2 (D24N, D44N, R45A) was used for the 2D IR measurements. The D44N is a physiological variant, seen in the Rostock form of the influenza A virus. This mutation increases the conductance of the channel approximately twofold, but otherwise it has properties very similar to wild-type.[45,46] The R45A mutation has minimal, if any, effects on the properties of the channel.[34] The residue D24, which was also mutated to N, is not a part of the transmembrane domain and therefore is not expected to influence drug binding and hydration of the pore.

III. RESULTS

A. Linear IR spectra

The linear IR spectra of M2 at pH values of 7 and 5 under three different experimental binding conditions, i.e., drug free, rimantadine bound, and spiran amine bound, are shown in Figure 2. The sharp band at ∼1672 cm^{-1} arises from residual TFA. The labeled amide transitions, at ∼1580 cm^{-1}, unfortunately do not offer enough signal to noise to allow for detailed analysis of lineshapes and their response to pH and drug binding in the channel. Moreover, linear infrared spectroscopy has significant limitations in revealing dynamics that

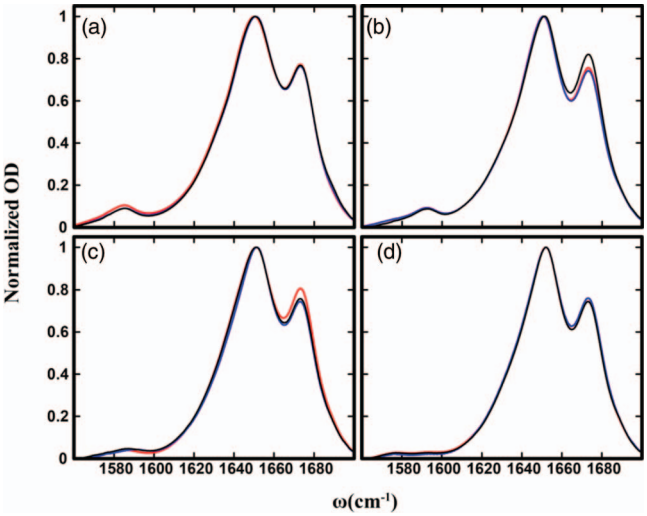

FIG. 2. Linear infrared spectra of isotopically labeled M2 channels obtained under different conditions: (a) Gly34 labeled M2 at pH 7, (b) Ala30 labeled M2 at pH 7, (c) Gly34 labeled M2 at pH 5, and (d) Ala30 labeled M2 at pH 5. For each case, the colors of the lines represent drug free (red), rimantadine bound (blue), and spiran amine bound (black) channels.

are underscored by the vibrational lineshapes; for the M2 channel, these dynamical timescales are characteristic to water structures near the pore lining amides as has been demonstrated before.[31] Thus, the remainder of this work focuses on the 2D spectroscopy of the isotopically labeled amides.

B. 2D IR spectra

The 2D IR spectra of amide modes of Gly34 and Ala30 at pH 7, in which the channel is closed, are shown in Figure 3 (for simplicity, only the spectral region corresponding to the absorption of the labeled amide is shown). It is clearly seen that neither the spectra of Ala30 nor those of Gly34 show any significant changes with increasing waiting time (i.e., T), as well as with the addition of the aforementioned drugs, indicating nominal changes in the water density and environment near the Ala30 and Gly34 amides. One noticeable difference between the spectra of Ala30 and Gly34 is that the Ala30 peak is blue-shifted by $\sim$5 cm^{-1} compared to the Gly34 band. Noting that backbone amide vibrational frequencies are susceptible to the electrostatic environment inside a protein,[30,47,48] the frequency difference between the Ala30 and the Gly34 bands is not unexpected, considering that the Ala30 residues are one turn further away from the charged His37 sidechains.

It has been shown that the vibrational lifetime reports on the interactions of a vibrator with surrounding water molecules.[32,49–51] However, it should be noted that the variation in the amide I vibrational lifetimes of proteins is generally small. For example, a change of $\sim$50% was observed between a solvated and a hydrophobic site in the M2 tetramer.[32] Despite the relatively small variation, this result suggests that the lifetime of the amide I vibration is sensitive to changes in the local solvent density.[32] As shown (Figures 4(a) and 4(b)), the amide I′ vibrational lifetimes of Ala30 and Gly34, which were determined by examining the decay of the respective 2D

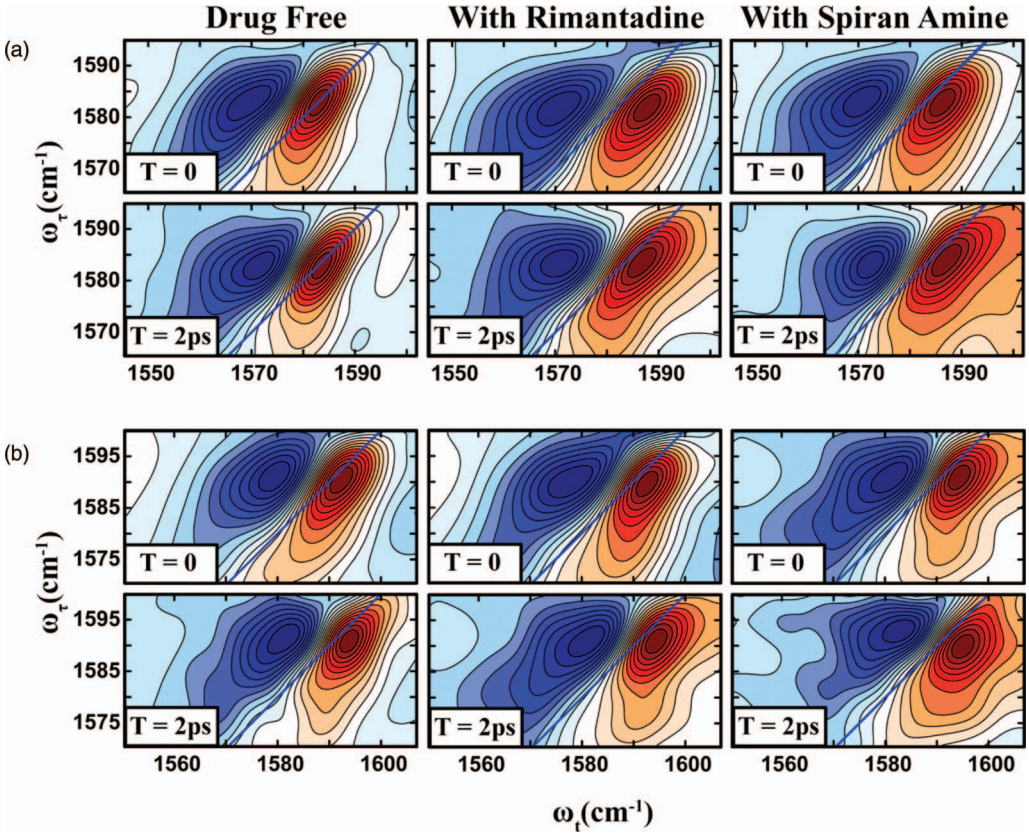

FIG. 3. 2D IR spectra of the amide I′ mode of isotopically labeled Gly34 (a) and Ala30 (b) at waiting times of 0 and 2 ps under different drug binding conditions at pH 7.0.

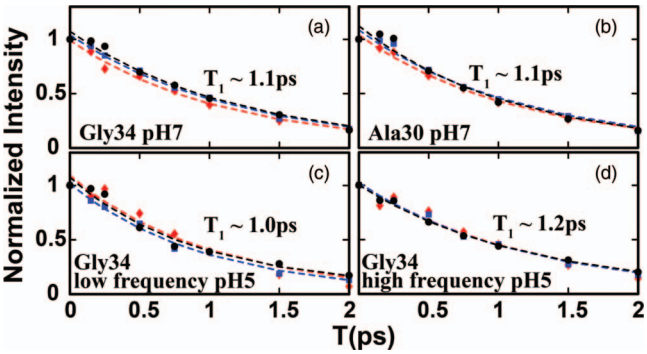

FIG. 4. Normalized 2D IR peak intensities versus waiting time T for the amide I′ modes of isotopically labeled Gly34 and Ala30 at pH 7 and 5 in the drug free (red squares), rimantadine bound (blue squares), and spiran amine bound (black circles) channels. For each case, the vibrational lifetime was estimated by fitting the respective data to an exponential decay (dashed line).

IR peak intensity with waiting time, are identical. In addition, these lifetimes show no measurable changes with addition of either one of the two drugs, indicating that there is no significant change in the water density near these residues, even upon drug binding. This is consistent with a model in which not all of the water is expelled from the pore upon drug binding.[23,27]

Lowering the pH to 5, which is the open state of the channel, causes the 2D IR spectra of Ala30 and Gly34 to split into doublets, as shown in Figure 5(a). The position of the stronger and higher frequency band at 1584 cm^{-1} is nearly the same as that observed for Gly34 at pH 7.0, while the lower frequency component is located at ∼1570 cm^{-1}. For the Gly34 spectra, the cross peak region between these bands exhibits a nonzero signal, which can arise from spectral overlap between the 2D lineshapes of the two modes or other mechanisms. However, the ratio of the cross-peak to diagonal-peak amplitudes does not show any significant waiting time dependence (data not shown), suggesting that in this case the cross peak does

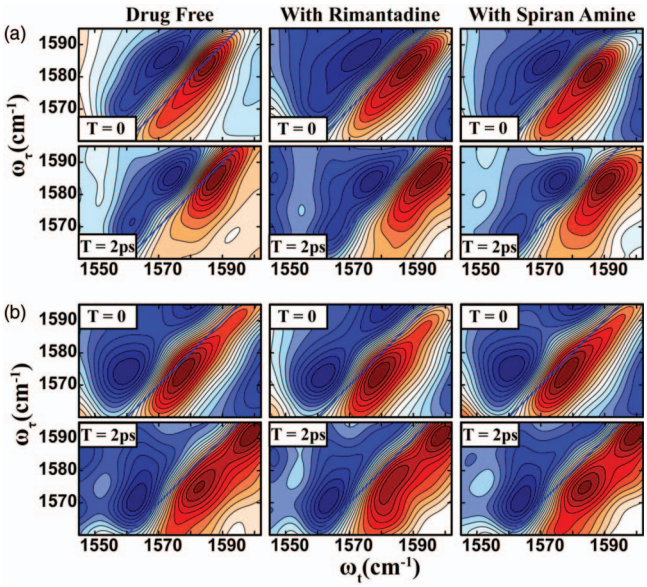

FIG. 5. 2D IR spectra of the amide I′ modes of isotopically labeled Gly34 (a) and Ala30 (b) at pH 5.0 and under different conditions, as indicated.

not arise from a population transfer or exchange process (see more discussion below). In addition, as shown in Figures 4(c) and 4(d), the difference between the vibrational lifetimes of these two modes is small, with the lower frequency bands exhibiting a slightly faster relaxation time constant (i.e., 1.0 ps compared to 1.2 ps). The invariance of T_1 under different drug binding conditions is also consistent with the observation at pH 7, and indicates no significant change in hydration upon drug binding near Gly34.

Similar to the Gly34 amide, at pH 5.0 the Ala30 band is also split into a doublet, located at ∼1574 cm^{-1} and ∼1590 cm^{-1}, respectively (Figure 5(b)). It is apparent that the high frequency component coincides with the Ala30 band observed at pH 7.0. However, contrary to that observed for Gly34, the low frequency component becomes, in this case, the more intense one, indicating that at this pH the amide groups of Ala30 and Gly34 experience different interactions with the surrounding waters. Furthermore, unlike that observed for Gly34, the intensity of the cross peak between the doublet increases with increasing waiting time (Figure 7), indicating equilibrium exchange between two distinct amide species. The evidence of exchange between these modes suggests that they do not represent different conformers of the channel, as it is extremely unlikely to have protein conformational transitions occurring on a timescale of ∼2 ps. Unfortunately, in the presence of such underlying dynamical equilibria, the 2D intensities undergo waiting time dependent modulations that are coupled to the vibrational relaxation; thus extracting vibrational lifetimes from the disappearance of the 2D signal is not possible without knowledge of the timescale of the exchange kinetics. However, as discussed later, the exchange timescale can be obtained under certain approximations, and provides valuable information on the dynamical processes that contribute to the aforementioned spectral evolution.

C. Probing water dynamics through amide frequency relaxations

It is well known that the motion of water molecules near an amide unit induces fluctuations in its vibrational frequency, causing the vibrational frequency correlation to decay on the timescale at which hydrogen bonds are formed and broken between the amide and water.[42,47] The decay of the frequency-frequency correlation function is reflected in the evolution of the corresponding 2D spectral shape with the waiting time. However, 2D lineshapes are often dominated by homogeneous and inhomogeneous contributions, and the waiting time evolution of the lineshape is not always apparent and easily quantifiable, such as in the current case. Therefore, we employed the integrated peak shift approach[52,53] to extract the underlying correlation dynamics from the experimental 2D IR data.[54] Specifically, integrated photon echo peak shift moments were evaluated from the 2D IR spectra by windowing the isotopically labeled amide bands to quantitatively assess the water dynamics,[52,53,55] using a spectral window of 20 cm^{-1} along ω_τ and 40 cm^{-1} along ω_t, respectively, to spectrally isolate the vibrational transitions of interest. The applicability of this method was tested through numerical

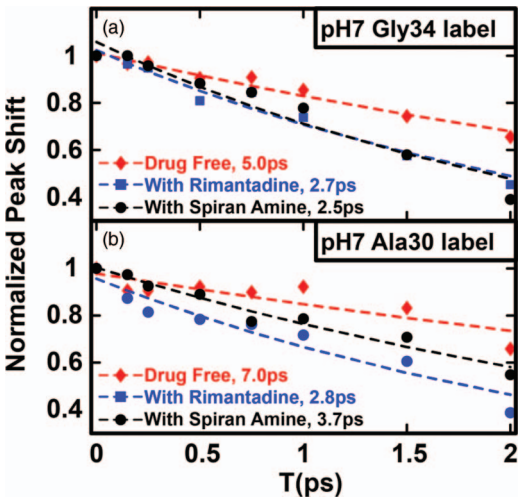

FIG. 6. Experimental integrated peak shifts of the isotopically labeled Gly34 and Ala30 amides at pH under different drug binding conditions, as indicated. The dashed lines represent fits to the experimental data. For each case, the experimental peak shifts were fitted to an exponential decay to obtain the frequency autocorrelation time τ_C.

simulations of 2D IR spectra, elaborated in the supplementary material.[56] The corresponding decay was fit to an exponential function, $P(T) = P_0 + P_1 e^{-T/\tau_C}$ to extract the frequency correlation time τ_C. As shown (Figure 6(a)), the τ_C values of Gly34 obtained under different drug-binding conditions at pH 7 indicate that drug binding affects its spectral diffusion timescale, with a trend that drug binding decreases the frequency correlation time. A similar trend is also observed for Ala30 (Figure 6(b)). At pH 7.0, in the closed state, both Ala30 and Gly34 in the drug free channel exhibit very slow spectral diffusion dynamics, indicating that the water structure near these sites is more ordered or even "*frozen*" on the timescale of our experiments, similar to that observed in ice crystals.[57] This is consistent with our prior experiments[33] and also MD simulations.[22,23] However, upon binding of a drug the water dynamics inside the channel become distinctively faster, as manifested by the faster spectral diffusion times of Al30 and Gly34. This fact suggests that the drug binds in the +2 state of the channel not by displacing the water clusters near these sites, but rather by disrupting or breaking their rigid structures. In bulk water, hydrogen bonds break and form on the timescale of ∼1 ps, which is reflected in the frequency correlation function of small solvated peptides.[47] The timescales measured here indicate that the drug increases the dynamics of the water in the channel, but the dynamics are still slower than in comparison to bulk water. The doublets observed for Gly34 and Ala30 at pH 5, however, make an accurate assessment of their spectral diffusion dynamics difficult, as it has been shown that for overlapping bands, the commonly used metrics, such as the center line slope, do not yield relaxation functions that represent the decay of the underlying frequency-frequency correlation function.[58] Fortunately, as shown in Sec. III D, the correlation dynamics can be evaluated by analyzing the cross-peak dynamics.

D. Solvent exchange between amide sites exposes drug-water interactions

The doublets observed at pH 5.0 (Figure 5) suggest the presence of either multiple conformations of the channel or different hydration/electrostatic statuses of the amide IR probe. However, a non-zero cross peak between these bands suggests that the states represented by these transitions are coupled, ruling out the possibility that they arise from two different conformers.[59] Given the fact that at pH 5.0 three of the four His residues are protonated, the splitting of the amide I′ bands of Ala30 and Gly34 most likely originates from an asymmetric charge distribution in the His37 tetrad, which would cause an asymmetric solvation of the pore lining amides, as protonated histidine strongly associates with water.[60] Since such a scenario would mandate a relative ratio of 3:1 or 1:1 between the two amide I peaks of Ala30 and Gly34, we evaluated this hypothesis by examining the diagonal traces of the corresponding 2D IR spectra at zero waiting time (i.e., $T = 0$). As shown in the supplementary material,[56] in each case the diagonal trace can indeed be fit adequately with two Gaussians with a ratio of 3:1. Thus, this analysis leads us to conclude that the doublet observed at pH 5.0 is indeed due to the asymmetric protonation of the His37 tetrad, which causes Ala30/Gly34 to sample two different local hydration/electrostatic environments. Interestingly, such an asymmetry was not observed in our prior experiments, where the occurrence of a doublet was attributed to separate conformers of the channel.[33] Thus, the possibility of the doublet arising from structural asymmetry that is inherent to the R45A mutant and not to the wild type cannot be ruled out.

The growth kinetics of a cross peak between two transitions can be used to reveal the timescale of the underlying equilibrium dynamics such as chemical exchange between two differently solvated chromophores.[61–64] Noting that for a vibrator in water, the major contribution to spectral diffusion arises from the making and breaking of hydrogen bonds with water, the cross peak growth timescales essentially report on the same physical process of solvent reorganization around the Ala30 amide and can be used to understand the drug induced changes to the channel water. As shown in Figure 7, where the growth of the ratio of the cross peak to the diagonal peak at lower frequency is plotted, a cursory inspection suggests that the cross peaks obtained at all three experimental conditions exhibit a growth time of less than 2 ps, which is

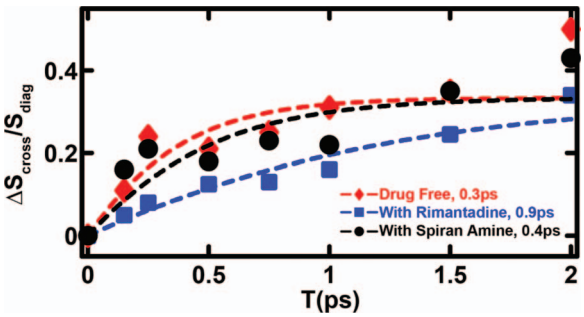

FIG. 7. Ratios of the cross peak to the lower frequency diagonal peak of the Ala30 doublet as a function of the waiting time under different drug binding conditions at pH 5.0, as indicated. The dashed lines represent fits to the two-state exchange model elaborated in the text.

consistent with previous reports on amide spectral diffusion in aqueous solutions.[47,51] A detailed treatment of the third order responses that contribute to the 2D IR signal for such a system in equilibrium has been presented elsewhere.[61,62] For such a two-state equilibrium process, the ratio of the diagonal and cross-peak signals in the 2D spectrum can be used to isolate the rate constants and thus the timescales for the exchange process. The ratio of the cross to the diagonal peaks can be written as

$$\frac{S_{AB}}{S_{AA}} = \frac{\mu_B^2 P_{AB}}{\mu_A^2 P_{AA}}, \tag{1}$$

where μ_i is the transition dipole moment of state i, and P_{AB} and P_{AA} are conditional probabilities given as

$$\begin{aligned} P_{AA} &= \mathbf{\Omega}\cosh(\mathbf{\Omega}T/2) + (K - 2k_A)\sinh(\mathbf{\Omega}T/2), \\ P_{AB} &= 2k_{AB}\ \sinh(\mathbf{\Omega}T/2), \end{aligned} \tag{2}$$

K and Ω are defined as

$$\begin{aligned} K &= k_A + k_B, \\ \mathbf{\Omega} &= [(k_A - k_B)^2 + 4k_{AB}k_{BA}]^{1/2}, \end{aligned} \tag{3}$$

where k_A and k_B are the total rates of relaxation from states A and B, respectively, while k_{AB} and k_{BA} represent the rates of hopping between states A and B. If we assume that the transition dipole strengths and the vibrational lifetimes of the two states involved are the same (which is reasonable, based on the T_1 values evaluated at pH 7), Eq. (1) can be simplified to

$$\frac{S_{AB}}{S_{AA}} = \frac{1 - e^{-2k_{ex}T}}{\frac{1}{K_{eq}} + e^{-2k_{ex}T}}, \tag{4}$$

where k_{ex} is the energy transfer rate, defined as $k_{ex} = \frac{k_{AB}+k_{BA}}{2}$, and K_{eq} is the equilibrium constant between states A and B. For the analysis of the cross peak evolutions from the 2D spectra of A30 at pH 5, the model outlined above was used to fit the ratio of the diagonal peak at 1574 cm^{-1} (state A) and the positive cross peak that appears between this band and that at 1591 cm^{-1} (state B). In keeping with the approach followed for the analysis of the diagonal traces, the equilibrium constant k_{AB}/k_{BA} was fixed at 1:3. To track only the growth of the cross peak signal with waiting time, the residual signal at $T = 0$ was subtracted from the data, thus yielding $\Delta S_{\text{cross}}/S_{\text{diagonal}}$. Fitting to the model described above (dashed lines in Figure 7) yields the exchange times for the drug-free, rimantadine-bound, and spiran amine-bound channels to be 0.3, 0.9, and 0.4 ps, respectively. Since that the forward and backward transfer rates are connected through the equilibrium constant, the rate k_{AB} can be calculated from the fitted exchange rates, which is $(0.6\ \text{ps})^{-1}$, $(1.9\ \text{ps})^{-1}$, and $(0.8\ \text{ps})^{-1}$ for the drug free, rimantadine bound, and spiran amine bound channels, respectively. Since experiments[47,51,55] and simulations[48] have revealed a timescale of ∼1 ps for hydrogen bond making and breaking for model amides in aqueous solution, these results are thus in accordance with the above mentioned idea that the doublet arises from different hydration/electrostatic states of the Ala30 amide in the same channel.

E. Channel water dynamics influences drug binding

The amide spectral diffusion and its response to drug binding at pH 7.0 reveals that the water structure near Ala30 and Gly34 is perturbed upon drug binding. MD simulations[23] predict a drug binding mechanism wherein the amino end of the drug is solvated by water molecules that are arranged in a square pyramidal geometry through hydrogen bonding interactions with Ala30 and Gly34 amide carbonyls. For such a binding mechanism, it is expected that the local hydration environments will show marked differences between the drug-free and drug-bound channels, as observed in the 2D IR measurements. Since the amide frequency fluctuation in this case is predominantly caused by making and breaking of hydrogen bonds between the labeled amide carbonyl and water, the fact that the drug-bound channels afford faster spectral diffusion dynamics not only supports the MD simulation results but also provides additional insights on the role of channel water in drug binding. More specifically, the spectral diffusion data are consistent with a water-mediated binding mechanism wherein the drug disrupts the ordered water structure near Ala30 and Gly34. Thermodynamically, this picture also makes sense[65] as the entropy gained from releasing the water molecules from a more rigid cluster would help stabilize the bound state of the drug.[66,67] While the overall binding mechanism involves a complex balance between enthalpic and entropic contributions, our results indicate that the increased translational entropy of the channel water presents a favorable factor in the thermodynamics of drug binding. Similar results have also been reported from experiments and MD simulations[68,69] where it has been suggested that the perturbation of well-ordered water molecules in protein binding sites upon ligand binding makes a favorable entropic contribution to the process. It is known that amantadine binding affinity to the channel is higher at neutral pH.[70] The timescale of ∼1 ps at pH 5 suggests a reduced entropic gain upon drug binding, thus providing a new insight toward the lower drug binding affinities in the 3+ state. In addition, and perhaps more interestingly, upon binding of rimantadine, the exchange rate is slowed down by about a factor of 2, whereas spiran amine binding has little effect on the exchange dynamics. However, it should be noted that the approximations invoked to simplify the model and also the relatively low signal-to-noise ratio in Figure 7 impose certain limitations on the accuracy of these timescales, and hence not the absolute exchange rates but their trends should be focused on. Since all the data were collected under identical experimental conditions, with the systems differing only with respect to the drug bound to the channel, these trends should reflect the change in the solvent dynamics local to the Ala30 residue.

These results are again in excellent agreement with MD simulations,[23] which predict that the amino moiety of amantadine interacts with the water cluster near Ala30 through hydrogen bond formation, which would slow down any exchange process that involves these water molecules, as observed. On the other hand, MD simulations predict that the amino group of spiran amine directly interacts with the water cluster near Gly34 and, thus, leaves the dynamics of water near Ala30 less perturbed. Noting that the MD simulations

were performed with pH 6.5 crystal structures, it is possible that the fast exchange dynamics observed herein reflect not merely a reorganization of solvent density around differently solvated backbone amides but also reorganization of the water near Ala30 in response to hopping and translocation of a proton between different sites. Considering the strong affinity for water of a protonated histidine,[60] and the proximity of Gly34 to the histidine tetrad, which allows water molecules to bridge between the glycine amide and the imidazole nitrogen,[28] it can be expected that the water near Gly34 is more ordered compared to that near the Ala30 site. This is reflected in the absence of any measurable solvent exchange at the Gly34 site. Taken together, we believe that the results obtained at both pH 7 and 5 support a binding mechanism wherein the amino end of the drug points toward the His37 tetrad and docks in its binding pocket through interactions with a nearby water cluster.

IV. CONCLUSIONS

In summary, we have employed 2D IR spectroscopy to gain new insight into the role of water in facilitating the binding of two amantadine-like drugs (rimantadine and spiran amine) to the influenza A virus M2 proton channel. By measuring the spectral diffusion of two isotopically labeled amide I′ vibrators, we are able to show that at pH 7.0, when the channel is in the +2 state, the water cluster near the pore-lining amides is in an immobilized, ordered state, which is perturbed upon binding of the aforementioned channel blocking drugs. These results suggest that the channel water gains entropy upon drug binding and thus acts favorably to stabilize the drug in its binding pocket at neutral pH. At pH 5.0, wherein the His37 tetrad is in its +3 state which favors diffusion of protons out of the channel, we find that the M2 channel affords more mobile water and hence a smaller entropic gain upon drug binding than at pH 7.0, which is consistent with the notion that the drug binding affinity is lowered at acidic pH. In addition, our results indicate an asymmetric distribution of water in the channel at pH 5.0, which is possibly connected to the charge distribution in the histidine tetrad. Taken together, we believe that these results highlight the importance of water in facilitating binding of channel-blocking drugs to the M2 channel, as well as, how site-specific dynamical and structural information revealed by 2D IR spectroscopy can be used to help provide a molecular level understanding of the drug binding mechanism.

ACKNOWLEDGMENTS

We thank the National Institutes of Health (Grant No. GM012592 to F.G. and Grant No. GM54616 to W.F.D.) for funding. The 2D IR data were collected at the Ultrafast Optical Processes Laboratory under Grant No. P41GM104605.

[1] M. Baz, Y. Abed, J. Papenburg, X. Bouhy, M. E. Hamelin, and G. Boivin, N. Engl. J. Med. **361**, 2296 (2009).
[2] E. De Clercq, Nat. Rev. Drug Discovery **5**, 1015 (2006).
[3] R. M. Pielak and J. J. Chou, BBA-Biomembranes **1808**, 522 (2011).
[4] J. Wang, J. X. Qiu, C. Soto, and W. F. DeGrado, Curr. Opin. Struct. Biol. **21**, 68 (2011).
[5] L. H. Pinto and R. A. Lamb, J. Biol. Chem. **281**, 8997 (2006).
[6] T. A. Cross, H. Dong, M. Sharma, D. D. Busath, and H. X. Zhou, Curr. Opin. Virol. **2**, 128 (2012).
[7] C. Wang, R. A. Lamb, and L. H. Pinto, Biophys. J. **69**, 1363 (1995).
[8] J. A. Mould, H.-C. Li, C. S. Dudlak, J. D. Lear, A. Pekosz, R. A. Lamb, and L. H. Pinto, J. Biol. Chem. **275**, 8592 (2000).
[9] A. L. Polishchuk, J. D. Lear, C. L. Ma, R. A. Lamb, L. H. Pinto, and W. F. DeGrado, Biochemistry **49**, 10061 (2010).
[10] J. Hu, R. Fu, K. Nishimura, L. Zhang, H. X. Zhou, D. D. Busath, V. Vijayvergiya, and T. A. Cross, Proc. Natl. Acad. Sci. U.S.A. **103**, 6865 (2006).
[11] D. Salom, B. R. Hill, J. D. Lear, and W. F. DeGrado, Biochemistry **39**, 14160 (2000).
[12] C. S. Gandhi, K. Shuck, J. D. Lear, G. R. Dieckmann, W. F. DeGrado, R. A. Lamb, and L. H. Pinto, J. Biol. Chem. **274**, 5474 (1999).
[13] M. Hong and W. F. DeGrado, Protein Sci. **21**, 1620 (2012).
[14] I. V. Chizhmakov, F. M. Geraghty, D. C. Ogden, A. Hayhurst, M. Antoniou, and A. J. Hay, J. Physiol. (London) **494**, 329 (1996).
[15] M. G. Yi, T. A. Cross, and H. X. Zhou, Proc. Natl. Acad. Sci. U.S.A. **106**, 13311 (2009).
[16] H. X. Zhou, Biophys. J. **100**, 912 (2011).
[17] L. H. Pinto, G. R. Dieckmann, C. S. Gandhi, C. G. Papworth, J. Braman, M. A. Shaughnessy, J. D. Lear, R. A. Lamb, and W. F. DeGrado, Proc. Natl. Acad. Sci. U.S.A. **94**, 11301 (1997).
[18] M. Sharma, M. G. Yi, H. Dong, H. J. Qin, E. Peterson, D. D. Busath, H. X. Zhou, and T. A. Cross, Science **330**, 509 (2010).
[19] F. H. Hu, K. Schmidt-Rohr, and M. Hong, J. Am. Chem. Soc. **134**, 3703 (2012).
[20] F. H. Hu, W. B. Luo, and M. Hong, Science **330**, 505 (2010).
[21] Y. Tang, F. Zaitseva, R. A. Lamb, and L. H. Pinto, J. Biol. Chem. **277**, 39880 (2002).
[22] V. Carnevale, G. Fiorin, B. G. Levine, W. F. DeGrado, and M. L. Klein, J. Phys. Chem. C **114**, 20856 (2010).
[23] J. Wang *et al.*, J. Am. Chem. Soc. **133**, 12834 (2011).
[24] S. D. Cady, K. Schmidt-Rohr, J. Wang, C. S. Soto, W. F. DeGrado, and M. Hong, Nature **463**, 689 (2010).
[25] J. Hu, R. Fu, and T. A. Cross, Biophys. J. **93**, 276 (2007).
[26] S. D. Cady, J. Wang, Y. B. Wu, W. F. DeGrado, and M. Hong, J. Am. Chem. Soc. **133**, 4274 (2011).
[27] R. X. Gu, L. A. Liu, Y. H. Wang, Q. Xu, and D. Q. Wei, J. Phys. Chem. B **117**, 6042 (2013).
[28] R. Acharya *et al.*, Proc. Natl. Acad. Sci. U.S.A. **107**, 15075 (2010).
[29] P. Mukherjee, I. Kass, I. Arkin, and M. T. Zanni, Proc. Natl. Acad. Sci. U.S.A. **103**, 8571 (2006).
[30] A. M. Woys, Y. S. Lin, A. S. Reddy, W. Xiong, J. J. de Pablo, J. L. Skinner, and M. T. Zanni, J. Am. Chem. Soc. **132**, 2832 (2010).
[31] A. Ghosh, J. Qiu, W. F. DeGrado, and R. M. Hochstrasser, Proc. Natl. Acad. Sci. U.S.A. **108**, 6115 (2011).
[32] J. Manor, P. Mukherjee, Y. S. Lin, H. Leonov, J. L. Skinner, M. T. Zanni, and I. T. Arkin, Structure **17**, 247 (2009).
[33] A. Ghosh, M. J. Tucker, and R. M. Hochstrasser, J. Phys. Chem. A **115**, 9731 (2011).
[34] X. Jing, C. Ma, Y. Ohigashi, F. A. Oliveira, T. S. Jardetzky, L. H. Pinto, and R. A. Lamb, Proc. Natl. Acad. Sci. U.S.A. **105**, 10967 (2008).
[35] Y. S. Kim and R. M. Hochstrasser, J. Phys. Chem. B **113**, 8231 (2009).
[36] Z. Ganim, H. S. Chung, A. W. Smith, L. P. Deflores, K. C. Jones, and A. Tokmakoff, Acc. Chem. Res. **41**, 432 (2008).
[37] A. W. Smith and A. Tokmakoff, Angew. Chem., Int. Ed. **46**, 7984 (2007).
[38] I. T. Arkin, Curr. Opin. Chem. Biol. **10**, 394 (2006).
[39] J. Marecek, B. Song, S. Brewer, J. Belyea, R. B. Dyer, and D. P. Raleigh, Org. Lett. **9**, 4935 (2007).
[40] I. V. Korendovych, Y. H. Kim, A. H. Ryan, J. D. Lear, W. F. DeGrado, and S. J. Shandler, Org. Lett. **12**, 5142 (2010).
[41] Y. S. Kim and R. M. Hochstrasser, J. Phys. Chem. B **109**, 6884 (2005).
[42] P. Hamm and M. T. Zanni, *Concepts and Methods of 2D Infrared Spectroscopy* (Cambridge University Press, Cambridge, New York, 2011).
[43] S. Bagchi, S. G. Boxer, and M. D. Fayer, J. Phys. Chem. B **116**, 4034 (2012).
[44] E. H. G. Backus, R. Bloem, P. M. Donaldson, J. A. Ihalainen, R. Pfister, B. Paoli, A. Caflisch, and P. Hamm, J. Phys. Chem. B **114**, 3735 (2010).
[45] V. Balannik, V. Carnevale, G. Fiorin, B. G. Levine, R. A. Lamb, M. L. Klein, W. F. DeGrado, and L. H. Pinto, Biochemistry **49**, 696 (2010).
[46] T. Betakova, F. Ciampor, and A. J. Hay, J. Gen. Virol. **86**, 181 (2005).
[47] A. Ghosh and R. M. Hochstrasser, Chem. Phys. **390**, 1 (2011).

[48]Y. S. Lin, J. M. Shorb, P. Mukherjee, M. T. Zanni, and J. L. Skinner, J. Phys. Chem. B **113**, 592 (2009).
[49]J. T. King, M. R. Ross, and K. J. Kubarych, J. Phys. Chem. B **116**, 3754 (2012).
[50]A. M. Woys, S. S. Mukherjee, D. R. Skoff, S. D. Moran, and M. T. Zanni, J. Phys. Chem. B **117**, 5009 (2013).
[51]M. F. DeCamp, L. DeFlores, J. M. McCracken, A. Tokmakoff, K. Kwac, and M. Cho, J. Phys. Chem. B **109**, 11016 (2005).
[52]P. Hamm, M. Lim, and R. M. Hochstrasser, Phys. Rev. Lett. **81**, 5326 (1998).
[53]D. G. Kuroda, J. D. Bauman, J. R. Challa, D. Patel, T. Troxler, K. Das, E. Arnold, and R. M. Hochstrasser, Nat. Chem. **5**, 174 (2013).
[54]S. T. Roberts, J. J. Loparo, and A. Tokmakoff, J. Chem. Phys. **125**, 084502 (2006).
[55]M. T. Zanni, M. C. Asplund, and R. M. Hochstrasser, J. Chem. Phys. **114**, 4579 (2001).
[56]See supplementary material at http://dx.doi.org/10.1063/1.4881188 for sample characterization, analysis of 2D diagonal traces, and fits of the vibrational lifetime and peakshifts.
[57]F. Perakis, S. Widmer, and P. Hamm, J. Chem. Phys. **134**, 204505 (2011).
[58]E. E. Fenn and M. D. Fayer, J. Chem. Phys. **135**, 074502 (2011).
[59]C. Kolano, J. Helbing, M. Kozinski, W. Sander, and P. Hamm, Nature **444**, 469 (2006).
[60]S. H. Li and M. Hong, J. Am. Chem. Soc. **133**, 1534 (2011).
[61]Y. S. Kim and R. M. Hochstrasser, Proc. Natl. Acad. Sci. U.S.A. **102**, 11185 (2005).
[62]K. Kwak, J. Zheng, H. Cang, and M. D. Fayer, J. Phys. Chem. B **110**, 19998 (2006).
[63]A. Ghosh, A. Remorino, M. J. Tucker, and R. M. Hochstrasser, Chem. Phys. Lett. **469**, 325 (2009).
[64]S. Woutersen, Y. Mu, G. Stock, and P. Hamm, Chem. Phys. **266**, 137 (2001).
[65]J. J. Prompers and R. Bruschweiler, J. Phys. Chem. B **104**, 11416 (2000).
[66]R. M. Davidson, A. Lauritzen, and S. Seneff, Entropy-Switz **15**, 3822 (2013).
[67]B. Bagchi, Chem. Rev. **105**, 3197 (2005).
[68]A. Biela, F. Sielaff, F. Terwesten, A. Heine, T. Steinmetzer, and G. Klebe, J. Med. Chem. **55**, 6094 (2012).
[69]S. Chiba, Y. Harano, R. Roth, M. Kinoshita, and M. Sakurai, J. Comput. Chem. **33**, 2210 (2012).
[70]C. Wang, K. Takeuchi, L. H. Pinto, and R. A. Lamb, J. Virol. **67**, 5585 (1993).